

Tin addition to improve the oxidation behaviour of Nb_{ss}/Nb₅Si₃ based in-situ composite

S.Knittel^a, S.Mathieu^b, M.Vilasi^c

Institut Jean Lamour - UMR7198, CNRS - Nancy-Université - UPV-Metz, France,

^astephane.knittel@lscsm.uhp-nancy.fr, ^bstephane.mathieu@lscsm.uhp-nancy.fr,

^cmicHEL.vilasi@lscsm.uhp-nancy.fr

Key words: Niobium, Silicides, Oxidation, Tin

Abstract. This work focuses on the effect of tin additions (2, 5 and 8%) to the MASC alloy (Nb-25Ti-8Hf-2Cr-2Al-18Si) on the microstructure and the oxidation behaviour at 815°C in air. The alloys are mainly constituted of a niobium solid solution plus the (α , β , γ) Nb₅Si₃ silicides. For the higher Sn additions (5 and 8%), a fourth phase is evidenced: it is enriched in Sn and has a crystal structure close to Nb₃Sn. The oxidation resistance of these alloys is clearly improved by tin additions: the oxygen inward diffusion is hindered and consequently the fragmentation of the silicides is avoided. Cracks in silicides are no longer observed for the MASC containing 8%Sn. This effect is not attributed to a better efficiency of the oxide scales but rather to the reduction of the niobium solid solution fraction with tin additions.

Introduction

High temperature applications require new categories of structural materials with high toughness and hot corrosion resistance in order to increase the operating temperatures. To date only nickel based superalloys are employed for such types of applications. Their operating temperature is limited to 1150°C because Ni-based superalloys lose their mechanical properties above this temperature. Presently, the improvement of such systems is very limited because of the vicinity of their melting points.

For higher temperature applications, metallic systems based on refractory metals are considered as candidates for replacing or complementing nickel-based alloys. Niobium alloys have received great attention because of their high mechanical properties and their lower densities (8.58) among the other refractory systems (Ni 8.91, Mo 10.2, W 19.35). Furthermore niobium exhibits a ductile to brittle transition at lower temperatures than molybdenum. Since the last ten years, niobium alloys are considered as a real potential material allowing the use of the refractory alloys in high temperature applications. High mechanical properties have been achieved with the developments of Nb_{ss}/Nb₅Si₃ based in-situ composites during the STREP European project ULTMAT (2004-2008).

However these alloys suffer from the *pest catastrophic oxidation* between 600 and 900°C which results in a rapid fragmentation of the alloys. Like the well-known MoSi₂ compound, the strengthening of Nb₅Si₃ phase is subjected to the pest phenomenon in this range of temperatures. Two works [1,2] report on the beneficial effects of tin additions in niobium in-situ composites resulting in delaying the pest phenomena. However the role of tin is not established.

For this study, niobium in-situ composites (Nb-25Ti-8Hf-2Cr-2Al-18Si = MASC alloy) are prepared by arc melting with tin additions of 2, 5 and 8at.%. The as-obtained microstructures are studied by metallographic analysis in order to determine the influence of tin content on the phase equilibria as well as on the evolution of phase compositions. Oxidation tests are carried out by thermo-gravimetric measurements at 815°C, temperature for which the alloys are very sensitive to the pest.

Experimental methods

Sample preparations. High purity powders (purity>99.9%) of Al, Cr and Sn were blended in an agate mortar and compacted under pressure at room temperature. The resulting pill was placed on a water cooled copper mould to be arc melted. The sample preparations were performed under inert argon atmosphere. Then small pieces of all the other Nb, Ti, Hf and Si elements were added to the Al-Cr-Sn sample to reach the desired compositions (Table 1). After three re-meltings, samples were finally cast to obtain a cylindrical ingot. The as-cast samples were then heat treated under vacuum for five days at 1200°C in order to assess the thermodynamic phase equilibrium. The ingots were then cut in disc-like shapes with 1 cm diameter and 1.5 mm thick.

Table 1: Alloys nominal compositions (in at.%)

Sample	Nb	Ti	Hf	Cr	Al	Si	Sn
MASC-2%	bal.	25	8	2	2	18	2
MASC-5%	bal.	25	8	2	2	18	5
MASC-8%	bal.	25	8	2	2	18	8

Microstructure characterisation. A Philips X'Pert Pro diffractometer was used with a θ - θ Bragg Brentano geometry and monochromatic $\lambda Cu_{k\alpha} = 1.5418 \text{ \AA}$ radiation associated with a fast X'cellerator detector to identify the main constitutive phases of the samples and their oxidation products. The crystal structure of each compound was identified by matching the characteristic XRD peaks against JCPDS data.

The metallographic observations were performed by scanning electron microscopy (SEM) using a Philips XL30 equipped with an energy dispersive X-ray spectrometer (EDX). The chemical compositions were determined using a Cameca SX100 microprobe by Wavelength Dispersive Spectrometry. Pure Nb, Ti, Hf, Cr, Al, Si, Sn and Cr_2O_3 for oxygen were used as standards for the quantitative analyses. The voltage and the current of beam were 15kV and 10nA, respectively. Under this voltage the spatial resolution was about $1\text{-}1.5 \mu m^3$. Thus, the EPMA punctual analyses were performed for phases of diameter higher than $5 \mu m$.

Oxidation tests. Before the oxidation treatment the samples were polished up to 2400 grid on SiC polishing paper, then cleaned ultrasonically in ethanol and dried. The oxidation tests were conducted using a SETARAM TAG 1750 symmetric thermobalance at 815°C in air.

Results and discussion

Microstructure characterisation of MASC-x%Sn. After the sample preparations and heat treatment processes, the samples were characterised by XRD, SEM and the compositions of the constitutive phases were assessed by EPMA. The XRD pattern of MASC-5%Sn is given as an example in Figure 1 and the identified phases for the three alloys are presented in Table 2.

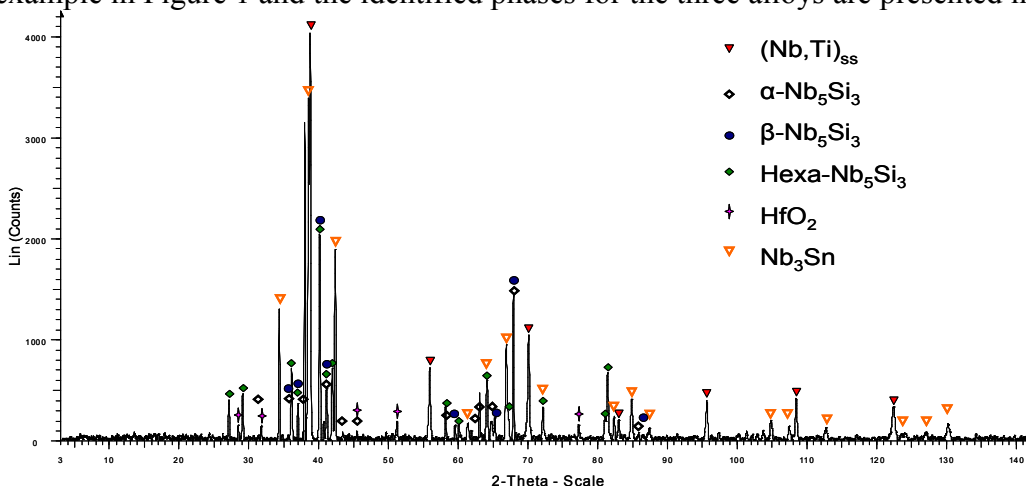


Figure 1: XRD pattern of MASC-5% after sample preparation and heat treatment.

Table 2: Phase detected on each sample by XRD(X present, - absent)

Sample	(Nb,Ti) _{ss}	β-(Nb,Ti) ₅ Si ₃	α-(Nb,Ti) ₅ Si ₃	γ-(Ti,Nb) ₅ Si ₃	HfO ₂	≈ Nb ₃ Sn
MASC-2Sn	X	X	-	X	X	-
MASC-5Sn	X	X	X	X	X	X
MASC-8Sn	X	-	X	X	X	X

Results of SEM and EPMA for the three alloys are given in Figure 2.

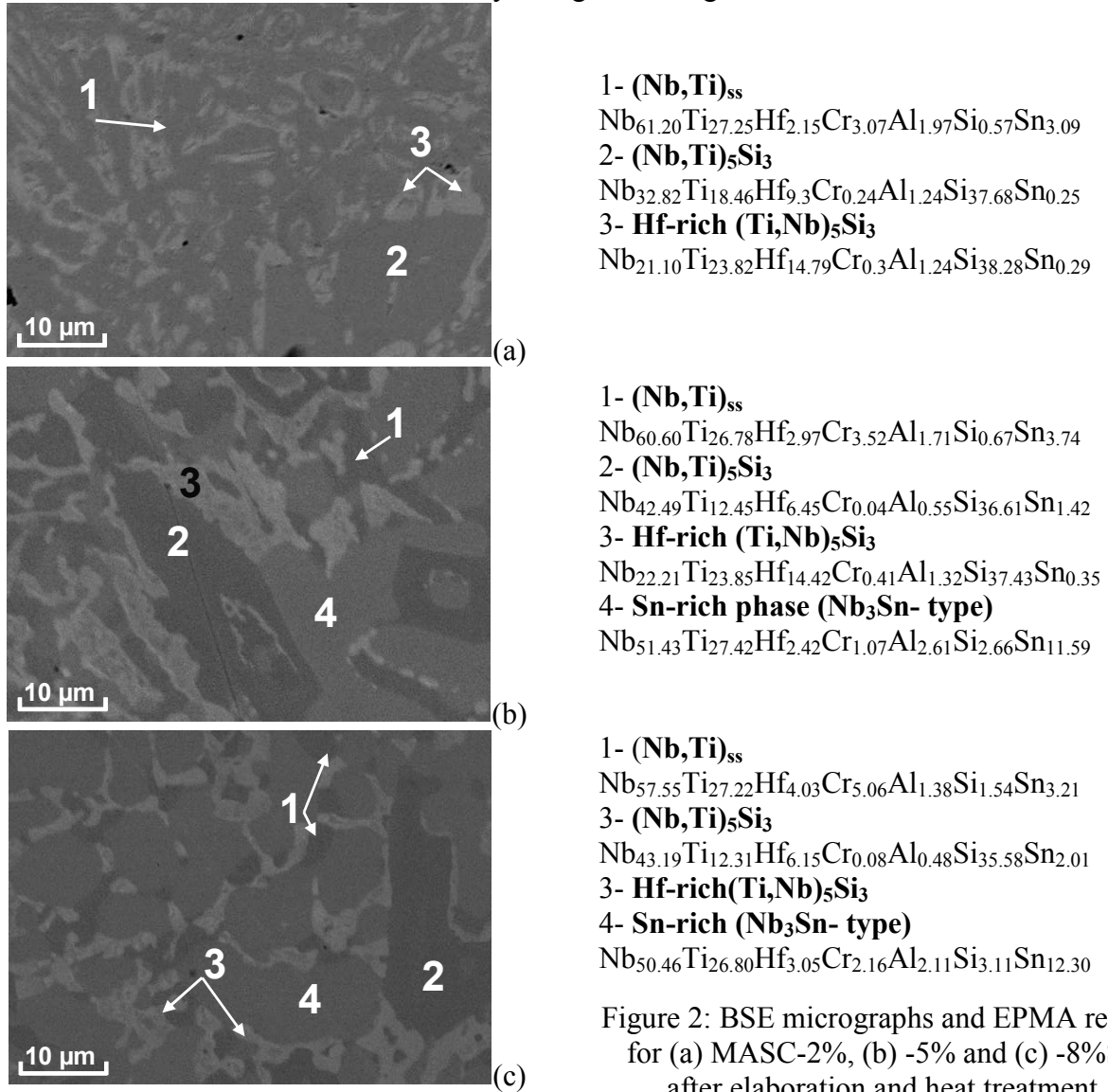


Figure 2: BSE micrographs and EPMA results for (a) MASC-2%, (b) -5% and (c) -8%Sn after elaboration and heat treatment

For MASC-2%Sn (Figure 2.a), the SEM observations exhibited mainly three phases, identified by examining/comparing both EPMA and XRD results: 1) a niobium rich solid solution (I $m-3m$) containing mainly Ti, small amounts of Hf, Cr, Al and 3%Sn; this phase is named hereafter (Nb,Ti)_{ss}. 2) the silicide Nb₅Si₃ with the β-high temperature cubic structure (I $4/mcm$ - prototype W₅Si₃) named hereafter (Nb,Ti)₅Si₃ and containing less than 10%Hf and 3) the Hf-rich (Ti,Nb)₅Si₃ with the γ-Ti₅Si₃ hexagonal structure ($P 6_3/mcm$ - prototype Mn₅Si₃) containing more than 10%Hf and also a higher titanium content than niobium. Geng *et al.* [3] reported previously that the γ-type phase is stabilized by hafnium. It should be noted that no Laves phase is observed in our case contrary to what was observed in [2]. Small particles of HfO₂ are also identified in all samples. For the MASC-5%Sn and MASC-8%Sn, the three phases observed for MASC-2%Sn are identified but for (Nb,Ti)₅Si₃ the two allotropic forms are observed, namely the β high temperature structure and the α-Nb₅Si₃ low temperature structure (I $4/mcm$ - prototype Cr₅B₃). For MASC-8%Sn, β-

Nb_5Si_3 is not evidenced and only the $\alpha\text{-Nb}_5\text{Si}_3$ is observed. Moreover a fourth Sn-rich phase is evidenced in MASC-5% and -8%. The phase has a cubic crystal structure ($P\ m3n$ - prototype Cr_3Si) and its lattice parameters are close to those of Nb_3Sn . According to the SEM micrographs, the higher the initial tin concentration, the higher is the volume fraction of the Sn-rich phase. In addition, this phase appears to gradually substitute the niobium solid solution. Consequently, the thermodynamic phase equilibrium evolves from $(\text{Nb},\text{Ti})_{\text{ss}} + \beta\text{-}(\text{Nb},\text{Ti})_5\text{Si}_3 + \gamma\text{-}(\text{Ti},\text{Nb})_5\text{Si}_3$ for low tin amounts to $\text{Nb}_3\text{Sn} + (\text{Nb},\text{Ti})_{\text{ss}} + \alpha\text{-}(\text{Nb},\text{Ti})_5\text{Si}_3 + \gamma\text{-}(\text{Ti},\text{Nb})_5\text{Si}_3$ for high Sn additions. The addition of tin has also several effects on the compositions of the MASC constitutive phases:

- First, EPMA data (Figure 2) shows that tin additions modify the solubility of the other elements within the $(\text{Nb},\text{Ti})_{\text{ss}}$. The addition of Tin is associated with an increase of the Hf, Cr and Si concentrations in the niobium solid solution. The alloying additions of the niobium solid solution decreases the solubility of tin (3.7 at.%) in bcc niobium as compared to 6at% in pure Nb at 1200°C according to the Nb-Sn binary [4]. Beyond 3.7 at.% the Sn-rich phase ($\approx\text{Nb}_3\text{Sn}$) is observed. Furthermore, the Ti and Al concentrations in $(\text{Nb},\text{Ti})_{\text{ss}}$ are not affected by the tin additions.

- The Hf and Ti concentrations of the $(\text{Nb},\text{Ti})_5\text{Si}_3$ decrease and in turn, increase in the Nb solid solution. In parallel, Sn (up to 2%) replaces silicon in the Nb solid solution".

- The composition of the Hf-rich $(\text{Ti},\text{Nb})_5\text{Si}_3$ compound does not seem to be affected at all by tin additions. However, this phase was impossible to analyse in the case of MASC-8%Al because its size is too small for accurate analyses.

Oxidation behaviour at 815°C of MASC-x%Sn. The oxidation behaviour of the three MASC alloys containing Sn was followed by thermogravimetric measurements for 100 hours at 815°C. The results obtained are given in Figure 3.

For the three samples, $\Delta m/S$ increases continuously with time and the shapes of the curves are not "stepwise" as observed by Geng *et al.*[2]. Mass gains remain low after 100 hours of exposure at 815°C and the total mass change decreases from 10.7 to 3.49 mg/cm² for MASC-2% and 8%, respectively. These values are in the same magnitude as those previously reported in [2].

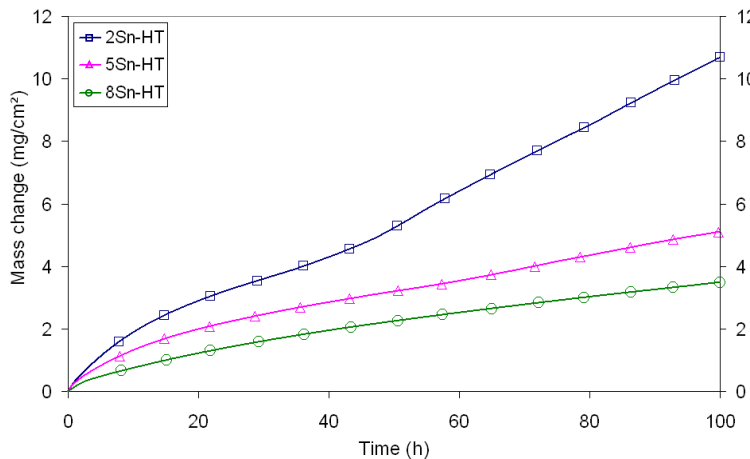


Figure 3: Thermogravimetric analyses of MASC-2, 5, 8%Sn for 100 hours at 815°C

The shape of the thermograms evolves when the Sn content increases. The kinetic treatment of the curves allows the assessment of the oxidation kinetics for each sample.

For the MASC-2%Sn, the mass gain increases with time following parabolic-like kinetics. The mass gain versus time curve follows a law of the type $\Delta m/S = \sqrt{2k_p t}$ with $k_p = 1.5 \times 10^{-10} \text{ g}^2 \cdot \text{cm}^{-4} \cdot \text{s}^{-1}$ for the first fifty hours of treatment, showing the limitation of the oxidation rate by diffusion in the solid state. This is followed by a linear kinetics with the associated linear constant k_l equals to $2.99 \times 10^{-8} \text{ g} \cdot \text{cm}^{-2} \cdot \text{s}^{-1}$.

If the tin content is increased, the oxidation kinetic slows down. MASC-5%Sn exhibits two oxidation steps similar to the sample containing 2%Sn: a first one which is parabolic for the first sixty hours ($k_p = 6.56 \times 10^{-11} \text{ g}^2 \cdot \text{cm}^{-4} \cdot \text{s}^{-1}$); a second one which is linear until the end of the experiment ($K_l = 1.11 \times 10^{-8} \text{ g} \cdot \text{cm}^{-2} \cdot \text{s}^{-1}$).

Finally, the MASC-8%Sn with the lower mass gain, also exhibits a parabolic kinetics throughout the 100hr of the oxidation test. The corresponding parabolic constant k_p is equal to $4.4 \times 10^{-11} \text{ g}^2 \cdot \text{cm}^{-4} \cdot \text{s}^{-1}$.

The increase of Sn content has consequently a positive effect on the mass changes in air at 815°C by reducing the oxidation rate. Furthermore, the linear and then rapid oxidation step is avoided by adding 8% tin, at least during 100h of treatment.

Microstructure characterisation of oxidised MASC-x%Sn. The XRD analyses of corrosion products formed on oxidised samples mainly reveal the presence of TiNb_2O_7 and also of TiO_2 and Nb_2O_5 in lower amounts. The characteristic peaks of TiO_2 rutile are identified on XRD patterns but they can also be attributed to CrNbO_4 which crystallises according to the same crystal structure. The nature of the formed oxides is not modified by the tin additions. The oxides developed on the sample are well adhered and no spallation is observed. The composition of the oxide scale determined by EPMA is also close to that of TiNb_2O_7 .

Figure 4 presents the SEM cross-section of the oxidised sample in back scattered electron mode.

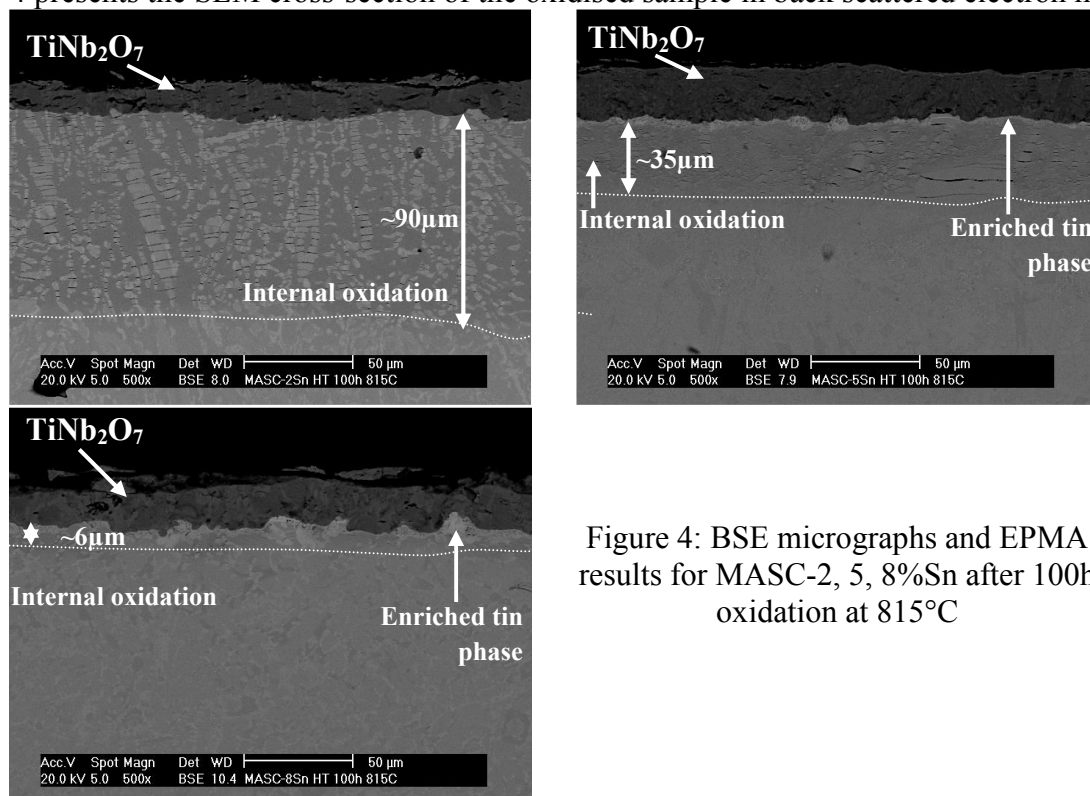


Figure 4: BSE micrographs and EPMA results for MASC-2, 5, 8%Sn after 100h oxidation at 815°C

The thickness of the oxide layer decreases as the tin concentration increases. This observation confirms the mass change evolution. Below the oxide scale, an internal oxidation zone can be observed; the internal oxidation mainly concerns the niobium solid solution. The depth of the oxygen penetration distinctly decreases with the increase of the tin concentration and changes from almost $100 \mu\text{m}$ for MASC-2%Sn to a few micrometers for the MASC-8%Sn. Fragmentation of silicides is observed for MASC-2 and 5%Sn but not for MASC-8%Sn.

A tin rich phase appears at the metal-oxide interface for the MASC-5% and 8%Sn during the oxidation treatment. Its amount increases with tin additions and an almost continuous sub-layer of this Sn-rich phase forms in the MASC-8% sample. The microprobe analyses do not allow the determination of an accurate composition of this Sn-rich phase because the thickness of the Sn layer was not large enough.

According to the oxidation results, the tin additions do not modify the nature of the oxides formed on the alloys surface but improve the overall oxidation resistance. As such, the beneficial effect of Sn has to be explained for assessing the oxidation mechanism.

For MASC alloys [5] oxidized at 800°C , the proposed oxidation mechanism indicates that the poor resistance (notably regarding pest phenomenon) of Nb/Nb₅Si₃ alloys is mainly due to the poor oxidation resistance of the niobium solid solution. Indeed, oxygen dissolves easily in the niobium

solid solution and leads to a high volume expansion of the Nb_{ss} phase. This induces a high stress level on the brittle niobium silicides nearby which fragment (and then pest) to relax the stresses. Thus, one of the key points to limit the rapid oxidation of niobium alloys is to reduce the niobium solid solution fraction in order to decrease the overall penetration of oxygen inside the alloy which is permitted by the high solubility of oxygen in niobium solid solution [6]. The present results obviously show that tin additions higher than 3.7% lead to the decrease of the niobium solid solution fraction and lead to the formation of the Nb₃Sn-type phase. The latter dissolves oxygen in a lesser degree than (Nb,Ti)_{ss} and therefore tends to limit the oxygen inward lattice diffusion. Moreover, it allows the formation of a Sn-rich phase below the oxide scale which 'plays the role' of a diffusion barrier for oxygen during the oxidation test. As a consequence, almost no internal oxidation is observed for the MASC-8%Sn and no fragmentation of silicides occurs.

Based on these promising results obtained on tin additions to Nb-Nb₅Si₃ at 815°C, future work will be focused on the study of the oxidation behaviour at high temperature (1200°C) in order to verify the persistence of the Sn beneficial effect.

Conclusions

The MASC alloys microstructure changes to a large degree with tin additions above 3.7at% that corresponds to the solubility limit of tin in the niobium solid solution. Beyond this value a Sn-rich phase with a crystal structure close to Nb₃Sn is observed. This phase substitutes the niobium solid solution and impacts dramatically the oxidation resistance of the alloy. The oxygen inward diffusion is hindered and consequently the fragmentation of the silicides is avoided. Cracks in silicides are no longer observed for the MASC containing 8%Sn.

Acknowledgments

The authors would like to thank Afidah Abdul Rahim for her advices and the scientific support of the European Ultmat consortium. They would like also to thank the common service of microscopy and microanalyses (SCMEM) of the Faculty of Sciences and Techniques of Nancy (France) for its help for microscopic observations.

References

- [1] B.P. Bewlay, M.R. Jackson, J.C. Zhao, P.R. Subramanian, A review of very-high temperature Nb silicide based composites, *Met. and Mat. trans.* Vol34A, p.2043-2052, Oct 2003
- [2] J.Geng, P; Tsakirooulos, G.Shao, A thermo-gravimetric and microstructural study of the oxidation of Nb_{ss}/Nb₅Si₃-based in situ composites with Sn additions, *Intermetallics*, p 1-12, 2006
- [3] J.Geng, P.Tsakirooulos, G.Shao, A study of the effects of Hf and Sn additions on the microstructure of Nb_{ss}/Nb₅Si₃ based in situ composites, *Intermetallics*, 1-8, 2006.
- [4] C.Toffolon, C.Servant, J.C.Gachon and B.Sundam, Reassessment of the Nb-Sn system, *Journal of phase equilibria*, Vol.23 N°2, 134-139, 2002.
- [5] F.Zamoum, Nouveau matériaux à base de niobium et de molybdène pour turbines aéronautiques : relations de phases et oxydation, élaboration de nouveaux revêtements, Thesis of Nancy University France, April 2008.
- [6] S. Knittel, S. Mathieu, R. Podor, M. Vilasi, A. Mesbah, M. François, A study of the effect of Al, Si and Ti on the high temperature oxidation behaviour of Nb-Ti-Hf-Cr-Al-Si in situ composites alloys, (to be published in *Oxidation of Metals*)